Journal of Colloid and Interface Science 402 (2013) 312–319

Contents lists available at SciVerse ScienceDirect

Journal of Colloid and Interface Science

www.elsevier.com/locate/jcis

New surfactant for hydrate anti-agglomeration in hydrocarbon flowlines and seabed oil capture

Minwei Sun [a], Abbas Firoozabadi [a,b,*]

[a] Reservoir Engineering Research Institute, 595 Lytton Avenue Suite B, Palo Alto, CA 94301, USA
[b] Yale University, 9 Hillhouse Avenue, New Haven, CT 06511, USA

ARTICLE INFO

Article history:
Received 6 December 2012
Accepted 22 February 2013
Available online 10 April 2013

Keywords:
Gas hydrates
Hydrate anti-agglomeration
Surfactants
Surface adsorption

ABSTRACT

Anti-agglomeration is a promising solution for gas hydrate risks in deepsea hydrocarbon flowlines and oil leak captures. Currently ineffectiveness at high water to oil ratios limits such applications. We present experimental results of a new surfactant in rocking cell tests, which show high efficiency at a full range of water to oil ratios; there is no need for presence of the oil phase. We find that our surfactant at a very low concentration (0.2 wt.% of water) keeps the hydrate particles in anti-agglomeration state. We propose a mechanism different from the established water-in-oil emulsion theory in the literature that the process is effective without the oil phase. There is no need to emulsify the water phase in the oil phase for hydrate anti-agglomeration; with oil-in-water emulsion and without emulsion hydrate anti-agglomeration is presented in our research. We expect our work to pave the way for broad applications in offshore natural gas production and seabed oil capture with very small quantities of an eco-friendly surfactant.

1. Introduction

The formation of gas hydrates with crystalline structures composed of small gas molecules trapped in water molecule cages, often blocks oil and natural gas flowlines, and may result in serious safety and environmental problems [1–3]. The failure of the dome to capture leaking oil in the recent Gulf of Mexico oil spill is perhaps the most well-known example of hydrate blockage [4].

There are two methods to address the undesirable aspects of hydrate formation in hydrocarbon flowlines. One is through thermodynamic inhibitors with large quantities (e.g. 10–60 wt.% in the aqueous phase) due to bulk phase property changes [2]. The other approach relies on changing surface properties with small chemical quantities, which are referred to as the low dosage (active component 0.1–2.0 wt.%) hydrate inhibitors (LDHIs), including kinetic inhibitors (KIs) and anti-agglomerants (AAs) [2,5]. KIs (e.g., polyvinylpyrrolidone and polyvinyl-caprolactam) may either delay the nucleation [6] or reduce the growth rate of the hydrate phase [7], or both [2,5]. KIs are generally ineffective at high subcoolings (e.g., >10 °C) which is often the case in deepwater. AAs become an attractive option when hydrates are in the form of small particles that allow slurry flow.

AAs are surfactants which contain a hydrophilic headgroup that binds to a hydrate particle surface and a hydrophobic tail that prevents hydrate particles from aggregating. The belief in the literature is that AAs produce water-in-oil emulsions which convert into hydrate particles [2,8–12]. In other words, without the oil phase, there is no known mechanism under which the anti-agglomeration mechanism can occur [11,12]. Typical AAs are quaternary ammonium salts (QAs), first developed by Shell in 1993 [13]. In a number of patents, the inventors suggested quaternary ammonium/phosphonium compounds that show anti-agglomeration in gas hydrate [13–16]. Tests were performed with the watercut (ratio of water to total liquids; volume basis) of 33% to a pressure of 78 bar. Later, Champion Technologies Inc used amide compounds as anti-agglomerants [17]. Testing included oil/brine (7.5 wt.% salt)/natural gas at 33% watercut; the AA dosage varied from 1% to 3%. In a recent work we have shown that the more eco-friendly biosurfactant rhamnolipids (Rh) can also be applied in such applications [18].

A major limitation in using AAs is that they become ineffective when the watercut is above 50% [18–22]. Recently Gao reports a newly developed AA inhibitor effective at watercuts as high as 80% due to the presence of a high concentration of salts (e.g., 7 or 11 wt.% NaCl brine) or a large amount of methanol (e.g.,

Abbreviations: AA, anti-agglomerant; LDHI, low-dosage hydrate inhibitor; KI, kinetic inhibitor; QA, quaternary ammonium salt; Rh, rhamnolipids.

* Corresponding author at: Reservoir Engineering Research Institute, 595 Lytton Avenue Suite B, Palo Alto, CA 94301, USA. Fax: +1 203 432 4387.

E-mail addresses: msun@rerinst.org (M. Sun), abbas.firoozabadi@yale.edu (A. Firoozabadi).

0021-9797/$ - see front matter © 2013 Elsevier Inc. All rights reserved.
http://dx.doi.org/10.1016/j.jcis.2013.02.053

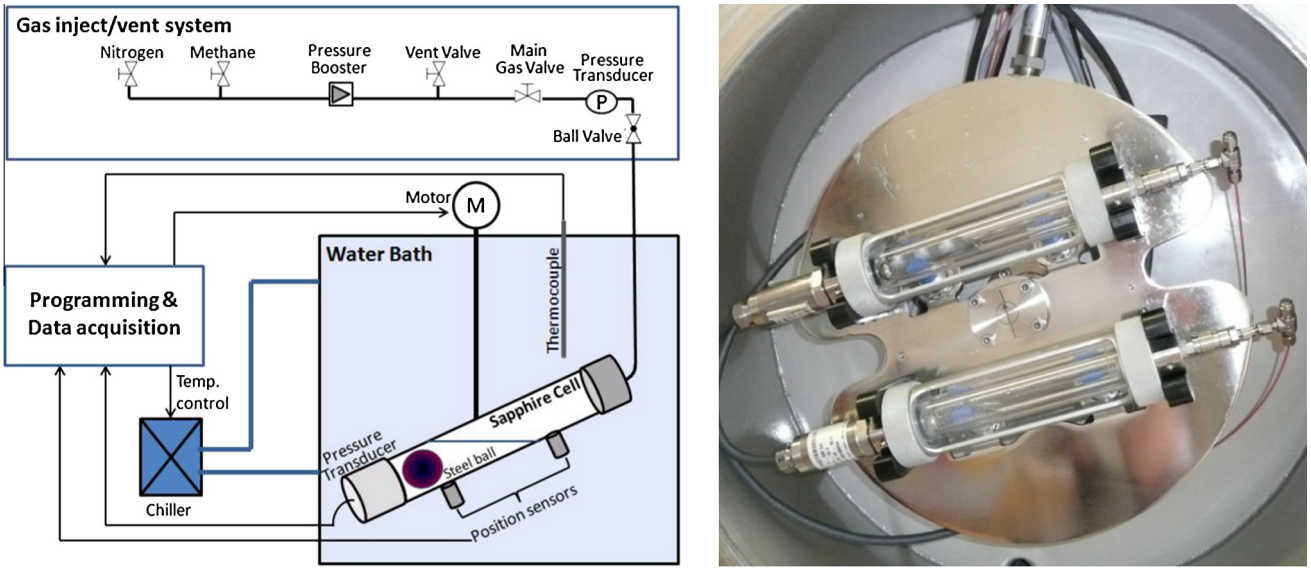

Fig. 1. Gas hydrate sapphire rocking cell setup.

15 wt.%). The addition of large amounts of salts or methanol are not practical for field applications [23]. To the best of our knowledge there are no reports of hydrate anti-agglomeration at 100% watercut, that is, without the oil phase. Even when the watercut is low, the toxicity and cost preclude the use of some of the AAs. As an example, QAs are not allowed in the North Sea due to environmental considerations regardless of their effectiveness [2]. The petroleum production industry has been looking for environmental friendly AAs for years, but little progress has been made to date for the conditions that there is no oil phase in sufficient amounts.

In this work we introduce a new AA which is effective even when there is no oil phase in the mixture. Our chemical solution contains cocamidopropyl dimethylamine (effective component) and glycerin. At a low dosage (e.g., 0.2 wt.% in the aqueous phase in most cases) it is an exceptionally effective anti-agglomerant in the full watercut range when there is no salt in the system. When the NaCl concentration is 4 wt.%, the special AA is effective at a dosage of 0.5 wt.% or less, in the aqueous phase in the full watercut range. We investigate the efficacy at watercuts ranging from 20% to 100% by mixing n-octane (oil) with the aqueous phase (water or brine). Pure methane, or a mixture of methane and nitrogen are employed as the gas phase. For comparison, PVP (polyvinylpyrrolidone, a KI), 2C-75 (a QA) and Rh are also examined. The tests are conducted in a customized RCS2 rocking setup (Fig. 1). We have also performed tests with crude oils instead of n-octane and the results are similar.

2. Material and methods

The experiments are performed in a sapphire rocking cell apparatus (by PSL Systemtechnik). Each cell has a volume of 20 mL equipped with a stainless steel ball to aid agitation. In each test, the cells are charged with 10 mL liquid samples, a mixture of the surfactant, n-octane (from Acros) and water or brine (4% NaCl). The water bath is filled before the cells are pressurized with a test gas to the desired pressure. We have set the rocking frequency from 10 to 30 times/min and seen no difference in results. It is set to be 15 times/min for most of the tests reported here. The bath temperature, the pressure and ball running time during rocking are recorded. Fig. 1 shows a schematic of the setup and an image of bath chamber with two sapphire cells installed. At the start after charging the cells with various fluids, they are rocked at 20 °C for half hour to reach equilibrium, which is set as initial condition of the closed cell test. Then the water bath is cooled from room temperature to 1 °C at different rates varying from −2 °C/h to −22 °C/h, while the cells are being rocked. They are then kept at 1 °C for a period of time allowing the gas hydrates to fully develop before the temperature ramps back to 20 °C. Sharp pressure changes indicate hydrate formation/dissociation. A long ball running time implies high viscosity in the cell. The steel ball stops running when hydrate plugging occurs. The effectiveness is evaluated by visual observations and by ball running time.

A tensiometer (K12, by Kruss) is used to measure the interfacial tension at 20 °C. Dynamic light scattering (ZetaPALS, by Brookhaven Instrument Corp.) is used to measure the size of the emulsions/aggregates in the liquid state at room temperature. Measurements are performed quickly after 2 min of hand-shaking at room temperature. Each measurement is completed in 30 s where the liquid mixture remains in the emulsion state. We repeat all the size measurements 10 times.

PVP-10 (from Sigma Aldrich) used in some of the tests has an average molecular weight of 10,000 g/mol, whose polydispersity is unknown. Arquad 2C-75 and Rh are used in comparison measurements [18–22]. The effective component in Arquad 2C-75 is quaternary ammonium compound, dicocoalkyl dimethyl chloride. Rh is a binary mixture, mono-rhamnolipid and di-rhamnolipid. The new AA (from Lubrizol Corporation) contains 80–89% cocamidopropyl dimethylamine (as the effective component), 5–10% glycerin, small amount of free amine and water. Glycerin and small amounts of amine and water are byproducts of surfactant synthesis. Since the concentration of these byproducts is very low (<0.05 wt.%) in this work, their thermodynamic effect is expected to be negligible. The chemical structures of the main components in the three AAs are shown in Fig. 2.

3. Results and discussion

3.1. Low to medium watercut range (20–50%)

We investigate anti-agglomeration state by varying the watercut from 20% to 50% at the AA concentration in the range of 0.1–0.5 wt.% in the aqueous phase. Results show that 0.1 wt.% is not sufficient at 50% watercut; plugging occurs soon after hydrate formation as seen in Fig. 3a, in which free liquid, gas and stainless

Cocamidopropyl dimethylamine:

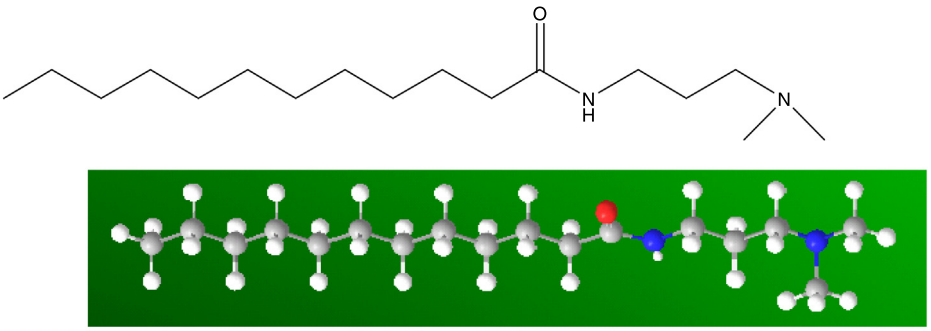

Rhamnolipids (Rh):

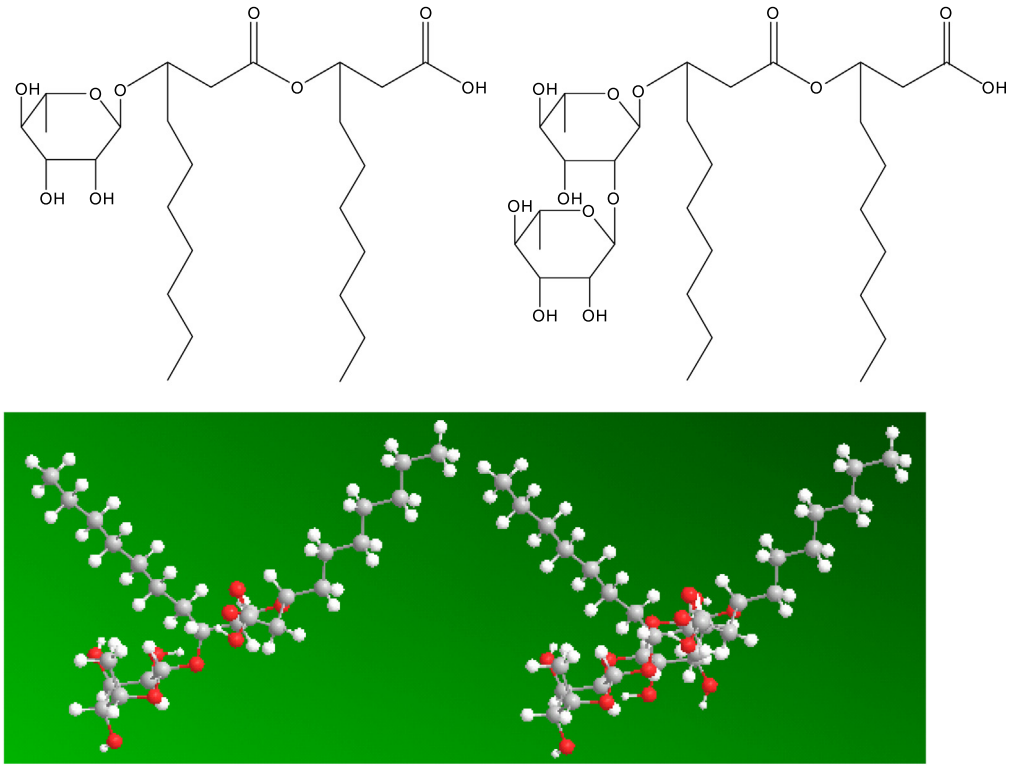

Arquad 2C-75:

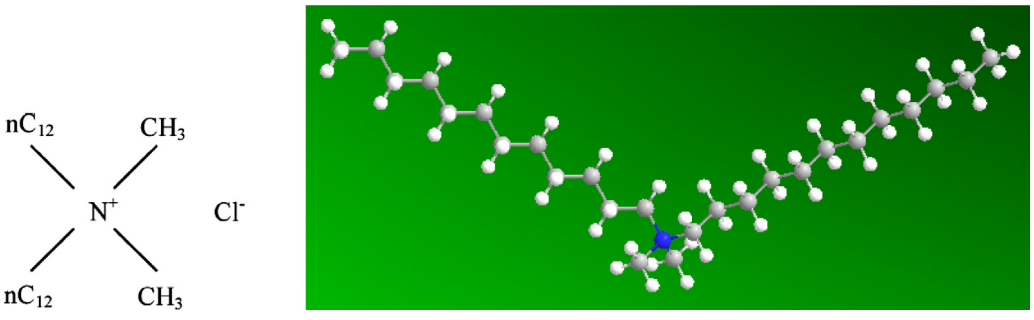

Fig. 2. Chemical structures (2D and 3D) of the main components in the three anti-agglomerants. Blue, red, grey and white spheres represent nitrogen, oxygen, carbon and hydrogen atoms. (For interpretation of the references to color in this figure legend, the reader is referred to the web version of this article.)

steel ball are all trapped in the ice-like hydrate. Once the AA dosage increases to 0.2 wt.%, there is no agglomeration at 50% watercut, as seen in Fig. 3b. The ball moves freely in the cell. The hydrate particles are carried by the free liquid. Fig. 4 presents the test results with methane at initial pressure of 140 bar. Methane hydrates form at 13 °C and pressure of 135 bar when 0.2 wt.% AA is added. The pressure in the cell drops to 81 bar at 1 °C and stays constant after all the water in the liquid mixture transforms into the hydrate. A 10 °C subcooling is established based on the equilibrium methane hydrate temperature of 11 °C at 81 bar. In the process

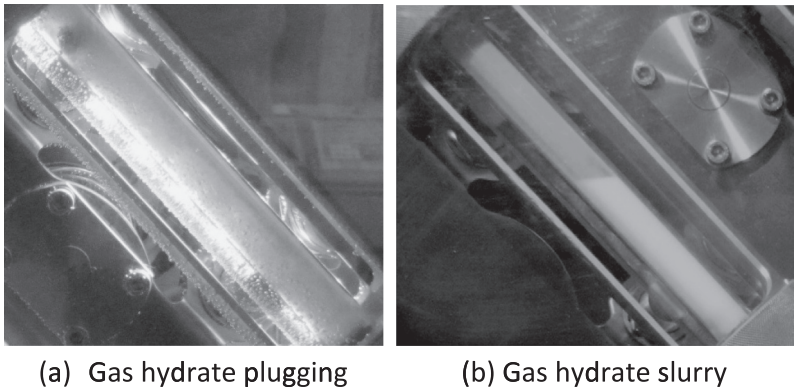

Fig. 3. Hydrate plugging at 0.1 wt.% AA (a) and hydrate slurry at 0.2 wt.% AA (b). The pictures are taken at 1 °C. Cooling rate is −2 °C/h from room temperature. The watercut is 50%.

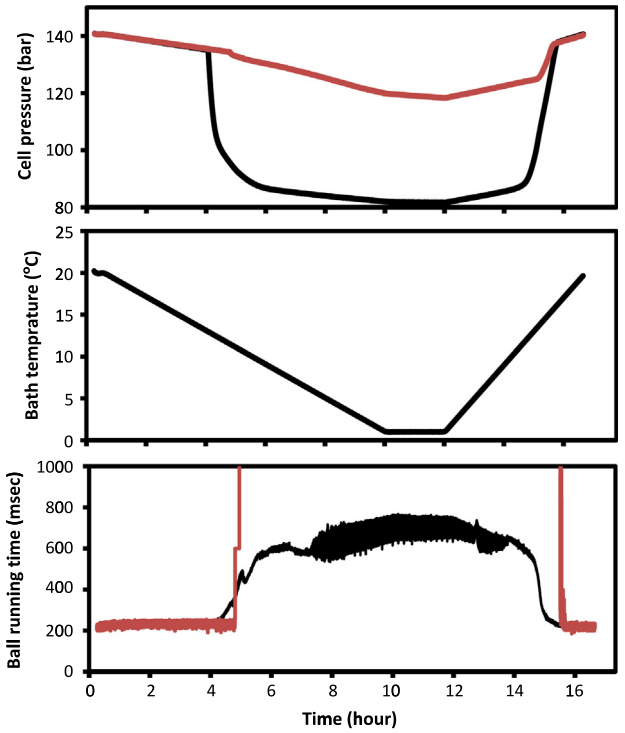

Fig. 4. Hydrate formation from the initial methane pressure of 140 bar at 20 °C. The temperature decreases from 20 °C to 1 °C at the rate of −2 °C/h, then kept at 1 °C for 2 h before ramping back to 20 °C. The concentration of AA (black) and PVP-10 (red) is both 0.2 wt.%. The watercut is 50%. (For interpretation of the references to color in this figure legend, the reader is referred to the web version of this article.)

of hydrate formation, the mixture turns into a slurry. The viscosity increases as indicated by the ball running time, increasing from 200 to 700 ms. The ball running time decreases from 700 back to 200 ms as the hydrate dissociates from temperature increase. During the temperature ramp to 20 °C, the methane hydrate dissociates at 12 °C and a pressure of 89 bar.

The red curves in Fig. 4 correspond to the test results from addition of 0.2 wt.% PVP-10. There is a 2 °C depression of hydrate formation temperature, which includes the kinetic inhibiting effect of PVP-10. However plugging occurs as soon as hydrate starts to form and the stainless steel ball stops running. In this test, methane is converted into hydrates slowly because the hydrate formation rate is limited by mass transfer. The hydrates block the communication of the liquid in the bottom part to the rest. The rate of pressure drop is very slow.

For comparison, tests with other AAs (2C-75 and Rh) are also conducted at 20%, 30%, and 50% watercuts at two different dosages (0.2 and 0.5 wt.%) at a cooling rate of −2 °C/h. In all the tests agglomeration is observed except for 2C-75 at 20% watercut. We have also investigated the kinetic inhibition effect of 1.0 wt.% PVP-10 at 50% watercut, which lowers the hydrate formation temperature by only 7 °C. This straightforward comparison demonstrates superiority of our AA.

3.2. High watercut range (60–100%)

Once the watercut is above 60%, the high volume fraction of hydrates in the liquid phase increases the viscosity of the mixture. Recently, Moradpour et al. have presented a model for predicting the emulsion–hydrate mixture viscosity in high watercut systems [24]. Fig. 5 shows the test with the watercut of 70% and AA dosage

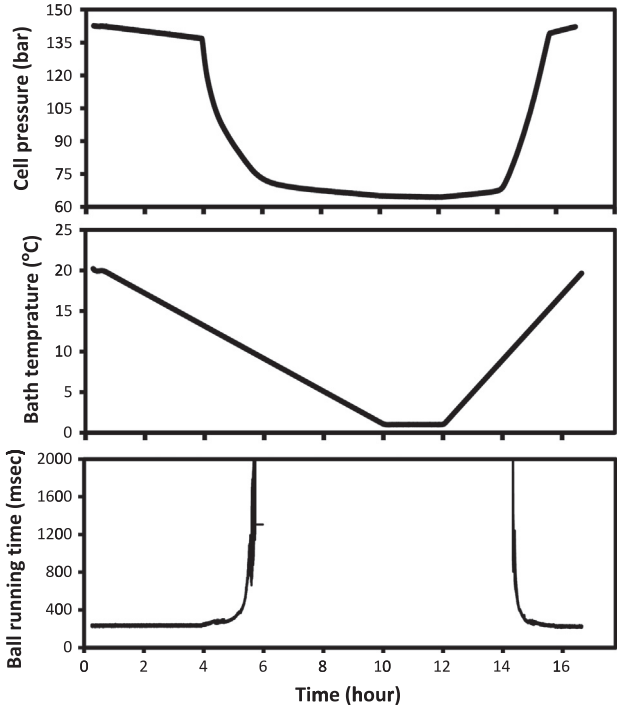

Fig. 5. Hydrate formation from the initial methane pressure of 142 bar at 20 °C. The temperature decreases from 20 °C to 1 °C at the rate of −2 °C/h, then kept at 1 °C for 2 h before ramping back to 20 °C. The concentration of AA is 0.2 wt.% and the watercut is 70%.

of 0.2 wt.%. Hydrates start to form at 13 °C at the pressure of 137 bar, and the hydrate content increases quickly as indicated by the sudden pressure drop. At 10 °C with pressure of around 78 bar, the ball running time spikes. Shortly afterwards, the ball running time is not recorded. We observe that the hydrate in the cell does not block the movement of the ball. The stainless steel ball moves very slowly in the hydrate slurry. Two pictures of the process are shown in Fig. 6. This interesting observation suggests that there is no plugging but there is a slurry of high viscosity because of the high hydrate content of about 24% by volume. The slurry may flow fast at high shear rate.

We use nitrogen in pressurization to reduce the high hydrate volume fraction in the liquid. We first introduce methane into the cells at 50 bar (equilibrium) and then add nitrogen to pressurize the cell to 160 bar (equilibrium). In this way, we control the volume of hydrates in the mixture to be less than 24%. We use our AA at 0.2 wt.% and the watercut is varied from 60% to 100%. Surprisingly anti-agglomeration is observed in all the tests even at a watercut of 100%. This is the first report of hydrate anti-agglomeration without the oil phase. As comparison, hydrate plugging occurs in all the tests if no AA is added at the same test conditions. Fig. 7 presents the successful result at 70% watercut. Hydrate starts to form at a temperature of 7 °C and a pressure of 153 bar. At 1 °C, the pressure drops to 102 bar. At this condition, the volume content of methane hydrate is about 21% in the liquid phase. The steel ball runs through the cell during the test while the ball running time increases from 200 ms to above 1000 ms when the hydrate content is high.

In addition to pressurizing the test cell, nitrogen gas also participates in the hydrate formation (sI hydrate as in methane). However, nitrogen can reduce the total amount of hydrates. For instance, in Fig. 5, the cell pressure decreases from 142 bar (20 °C) to 63 bar (1 °C) – a 79 bar drop; and in Fig. 7, the cell pressure decreases from 160 bar (at 20 °C) to 102 bar (at 1 °C) – a 58 bar drop. The molar fraction of nitrogen in the hydrate can be as high as 69% (methane 31%) estimated from the distribution coefficient method [12]. There is no agglomeration when we first introduce methane to 60 bar and then increase the pressure to 160 bar by nitrogen at watercuts from 60% to 100%.

3.3. Effect of cooling rate

We also investigate the effectiveness of AA in a wide range of cooling rates, a key factor for applications. In flowlines, the temperature drops slowly during transportation. However, the temperature decreases much faster in shut-in conditions and in the

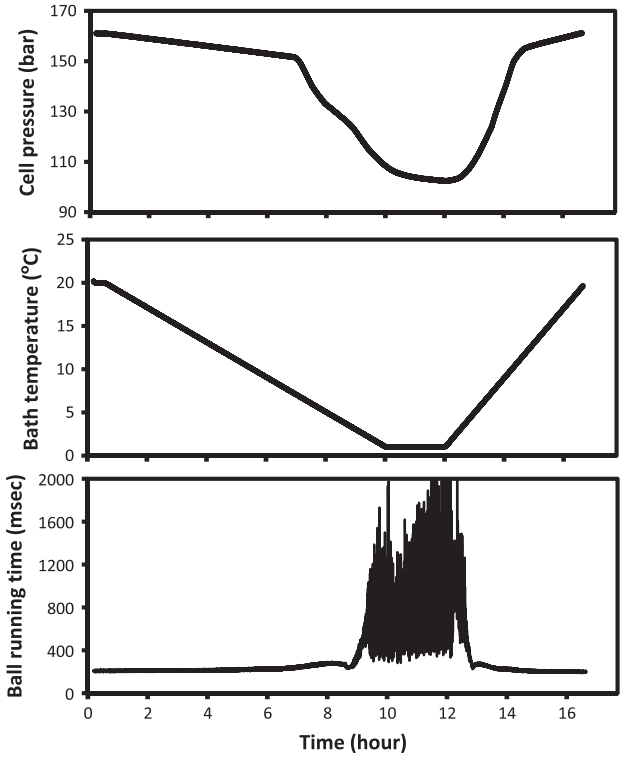

Fig. 7. Hydrate formation in tests in which methane is introduced to the cell at 50 bar and then by nitrogen the pressures is increased to 162 bar at 20 °C. The temperature decreases from 20 °C to 1 °C at the rate of −2 °C/h, then kept at 1 °C for 2 h before ramping back to 20 °C. The concentration of AA is 0.2 wt.% and the watercut is 70%.

conditions for oil capture in deepwater when the oil/gas mixes with cold sea water. We perform tests at cooling rates of −2, −10, and −22 °C/h. The effective dosages are shown in Table 1. At the low cooling rate of −2 °C/h, 0.2 wt.% AA is effective in the entire watercut range. However, when the cooling rate increases to −10 °C/h, a higher dosage is required in some cases. The increase may be due to the higher hydrate formation rates since the binding of AA molecules onto hydrate particle surfaces is a kinetic process. Interestingly there is no increase in AA dosage at high watercuts (e.g., from 80% to 100%), because of the mechanism which will be discussed shortly. From the cooling rate of −10 to −22 °C/h, we see no further dosage increase.

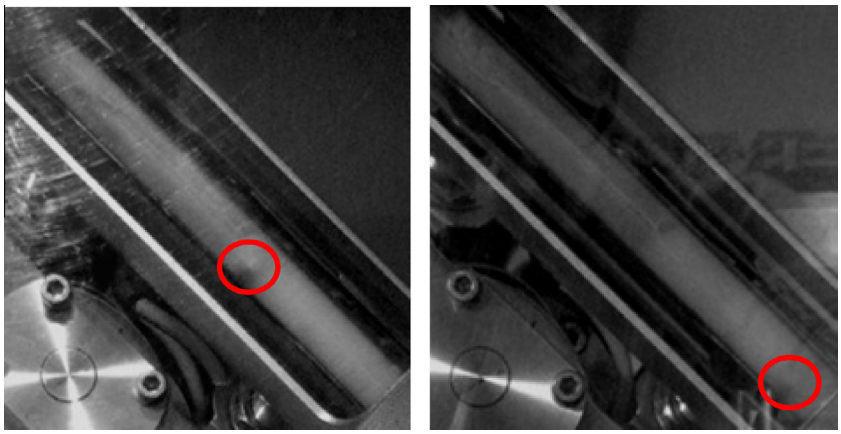

Fig. 6. Illustration of the movement of the stainless steel ball in high watercut conditions in the hydrate slurry. The right picture is taken 15 min later than the left picture by keeping the cell still at 1 °C. The red circles show the position of stainless steel ball.

Table 1
Effective AA dosage in methane/n-octane/water (and 4% NaCl brine) at different cooling rates.

Watercut (%)	Effective AA dosage (wt.%) methane/n-octane/water			Effective AA dosage (wt.%) methane/n-octane/brine		
	2 °C/h	10 °C/h	22 °C/h	2 °C/h	10 °C/h	22 °C/h
20	0.2	0.4	0.4	0.4	0.5	0.5
30	0.2	0.4	0.4	0.4	0.4	0.4
50	0.2	0.4	0.4	0.4	0.4	0.4
70	0.2	0.4	0.4	0.3	0.3	0.3
80	0.2	0.2	0.2	0.3	0.3	0.3
95	0.2	0.2	0.2	0.3	0.3	0.3
100	0.2	0.2	0.2	0.2	0.2	0.2

For applications in oil capture and in oil flowlines, there is salt in the aqueous phase. We use 4 wt.% NaCl brine (sea water concentration is 3–4 wt.%) to study the effect of salinity on anti-agglomeration. We tested the dosage by different levels, e.g., 0.1 wt.%, 0.15 wt.%, 0.2 wt.%, 0.3 wt.%, 0.4 wt.%, 0.5 wt.%, and 1.0 wt.%. As shown in Table 1, at −2 °C/h cooling rate, the effective dosages are either 0.3 or 0.4 wt.% except 0.2 wt.% at 100% watercut. A higher dosage is required compared to fresh water systems, which is probably due to the adsorption competition between electrolytes and surfactant molecules on the hydrate particle surface. Electrolytes usually enhance the adsorption of ionic surfactant [2,25], but may reduce the adsorption of nonionic surfactant [26]. A similar salt effect has been observed in our past work when using nonionic surfactant Rh [20]. Sloan and co-workers also found that the performance of PVCap was negatively impacted by methanol and a low slat concentrations (<5.5 wt.%) of salt [27]. Our AA molecules are highly effective at high watercuts in brine systems. Such remarkable effectiveness is desired in the applications where the watercut changes over a wide range (e.g., deepwater oil spill capture).

3.4. Proposed mechanism

In the past, the formation of water-in-oil emulsions has been proposed as a requirement in hydrate anti-agglomeration [2,8–12]. This hypothesis has been reinforced by lack of success in hydrate anti-agglomeration in methane/water systems. In this work, we find that our AA at 0.2 wt.% is effective in 100% freshwater or brine. There is neither the need for the oil nor emulsion formation.

The interfacial tension measurements are shown in Fig. 8. With no additive, the interfacial tension between n-octane and water is 50.8 mN/m at 20 °C. The introduction of 0.2 wt.% of our special AA reduces the interfacial tension dramatically to 5.6 mN/m. Rh and 2C-75 have a higher interfacial tension, 6.4 mN/m and 6.9 mN/m respectively. All these three AAs lower the interfacial tension significantly, however no significant difference is observed in their interfacial tension reduction power, which indicates that the interfacial tension reduction may not be the sole measure of AA effectiveness. PVP is not surface active as indicated by the interfacial tension of 47.3 mN/m. Dynamic light scattering measurements (Table 2) show that our special AA forms much smaller emulsions than 2C-75 and Rh in both 50% and 70% watercuts. It is unclear whether there is a correlation between emulsion size and effectiveness. A better understanding can be achieved when the hydrate particle size is measured. At room temperature and ambient pressure, we observe water-in-oil emulsions at 30% watercut. We observe oil-in-water emulsions when the watercut is above 50% and AA concentration is 0.2 wt.%. It should be noted that such emulsion is unstable as phase separation occurs in minutes. Such results demonstrate that stable emulsion is not necessary for anti-agglomeration as we discussed in the previous work [18], which is different from the well-established relatively stable water-in-oil emulsion theory [12]. The emulsion inversion is affected by many factors, e.g., temperature, oil phase, surfactant chemistry and amount, water to oil ratio, etc. We also measure the critical micelle concentration (CMC) of our AA in water by surface tension measurements as presented in Fig. 9, which is about 30 ± 3 ppm, much lower than the effective dosage of 2000 ppm. The CMC of Arquad 2C-75 and Rh are 7 ± 1 ppm and 18 ± 2 ppm respectively. There seems to be no correlation between the CMC and effectiveness of anti-agglomeration.

Table 2
Emulsion sizes of n-octane/water/AA (0.5 wt.%) at different watercuts at 20 °C.

Watercut (%)	Special AA (nm)	2C-75 (nm)	Rh (nm)
0	–	30.3 ± 4.9	3.8 ± 0.9
50	52.8 ± 3.7	124.2 ± 13.6	494.3 ± 35.0
70	14.8 ± 1.5	212.7 ± 50.6	385.3 ± 97.8
100	9.8 ± 1.4	23.3 ± 3.2	10.8 ± 1.6

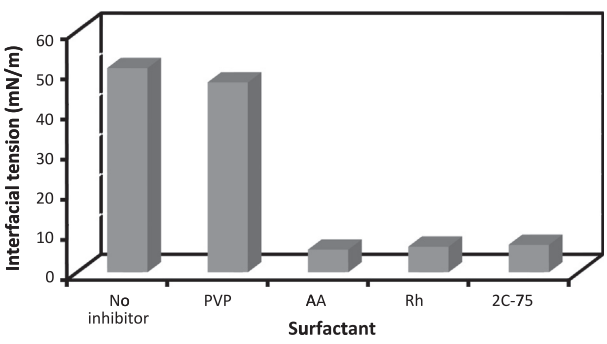

Fig. 8. The interfacial tensions between n-octane and water with different hydrate inhibitors at 50% watercut and at 20 °C. Inhibitors include PVP, our special AA, Rh and 2C-75.

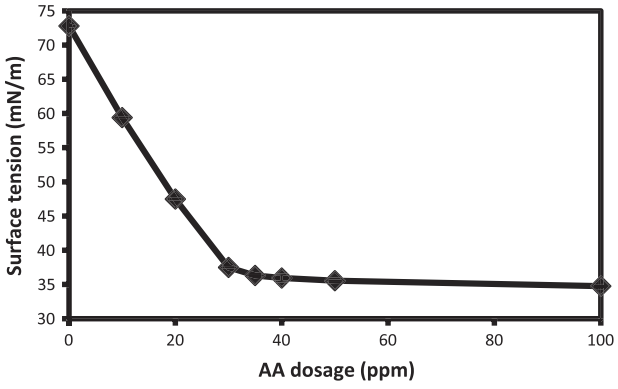

Fig. 9. The surface tension vs AA dosage for our chemical at 20 °C.

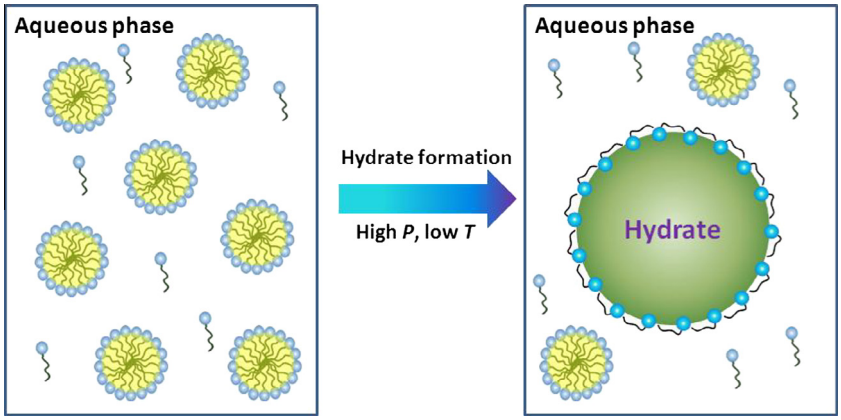

Fig. 10. Proposed mechanism in methane/water system.

In water, the surfactant molecules are mostly in the form of micelles as sketched in the left cartoon in Fig. 10. Once hydrate particles form in the mixture, some of micelles dissociate and the surfactants adsorb onto the hydrate particle surface. The dielectric constant of methane hydrates at 273 K is 58 [12], less than the 88 of water, which implies that the tail of the surfactant has more affinity for the hydrate surface. The tail may cover the hydrate surface as sketched in the right cartoon in Fig. 10. When there is adequate oil in the system the surfactant tail extends into the oil phase to provide steric repulsion between hydrate particles. In this case there is need for higher concentration of AA compared to the case when there is no oil, or when there is oil-in-water emulsion. Comparison of molecular architectures (Fig. 2) of our AA, Rh and 2C-75 indicates that the alkyl tail has the flexibility to cover the hydrate surface when the head is adsorbed in case there is no oil in the system. The alkyl tail in Rh is much shorter (C7 compared to C12 in our new AA), thus lacking the functionality to cover the hydrate surface. The hydrophilic headgroup of our AA may bind more strongly onto the hydrate surface than Rh or 2C-75. N···H–O hydrogen bond is stronger than O···H–O evidenced by the enthalpy of 29 kJ/mol vs 21 kJ/mol [28]. Our AA has two nitrogen and one oxygen hydrogen-bond acceptors in the headgroup; 2C-75 has only one nitrogen acceptor; and Rh has several scattered oxygen acceptors. The adsorption of surfactants at the liquid–solid interface may be a key [29]. We have begun a comprehensive molecular modeling to shed light on improved understanding of anti-agglomeration in hydrate systems. Results will appear in the literature as they become available.

4. Conclusions

We have demonstrated the superiority of our new AA over others surfactants – a low effective dosage over the entire watercut range at various cooling rates. The effectiveness of the anti-agglomerants reported by various authors in the past has not been shown at high watercuts. There is no claim in the literature of an anti-agglomerant which is effective without the oil phase. A recent book by Sloan and Koh [12] summarizes the common belief in the literature stating that "emulsifying the water phase in a liquid hydrocarbon phase" is the basis of anti-agglomeration. We have presented results showing that one may have anti-agglomeration without the oil phase, or when there is oil-in-water emulsion at high watercuts.

This work has a strong implication to environmental stewardship in hydrocarbon energy production. The use of large quantities of methanol in hydrate inhibition has raised safety concerns [30]. Because of effectiveness, the amount of our chemical is much lower compared to many other chemicals. Our AA has also lower toxicity compared to QAs [2]. The use of the surfactant introduced in this work has the potential to eliminate the risk of hydrate blockage in offshore gas flowlines, and to capture the oil from deepwater spill.

The effectiveness of our AA at 100% watercut cannot be explained by traditional water-in-oil emulsion theory [2,8–12]. We propose a new mechanism based on the micelle formation and equilibrium among the adsorbed surfactants on the hydrate interface, the dispersed molecules and the micelles in the aqueous phase. Hydrate anti-agglomeration can also occur in oil-in-water emulsion.

This work paves the way for use of a new class of AAs in hydrocarbon energy production, especially in offshore gas production.

Acknowledgment

We thank the member companies of the Reservoir Engineering Research Institute (RERI) for their financial support.

References

[1] C.A. Koh, R.E. Westacott, W. Zhang, K. Hirachand, J.L. Creek, A.K. Soper, Fluid Phase Equilibria 194 (2002) 143–151.
[2] M.A. Kelland, Energy & Fuels 20 (3) (2006) 825–847.
[3] M. Wu, S. Wang, H. Liu, Journal of Natural Gas Chemistry 16 (1) (2007) 81–85.
[4] B. Graham, W.K. Reilly, F. Beinecke, D.F. Boesch, T.D. Garcia, C.A. Murray, F. Ulmer, Deep Water: The Gulf Oil Disaster and the Future of Offshore Drilling (Report to the President), 2011.
[5] S. Mokhatab, R.J. Wilkens, K.J. Leontaritis, Energy Sources Part A – Recovery Utilization and Environmental Effects 29 (1) (2007) 39–45.
[6] D. Kashchiev, A. Firoozabadi, Journal of Crystal Growth 250 (3–4) (2003) 499–515.
[7] D. Kashchiev, A. Firoozabadi, Journal of Crystal Growth 241 (1–2) (2002) 220–230.
[8] Z. Huo, E. Freer, M. Lamar, B. Sannigrahi, D.M. Knauss, E.D. Sloan, Chemical Engineering Science 56 (17) (2001) 4979–4991.
[9] E.D. Sloan, Fluid Phase Equilibria 228 (2005) 67–74.
[10] M.L. Zanota, C. Dicharry, A. Graciaa, Energy & Fuels 19 (2) (2005) 584–590.
[11] A.P. Mehta, P.B. Hebert, E.R. Cadena, J.P. Weatherman, Old Production & Facilities 18 (1) (2003) 73–79.
[12] E.D. Sloan, C.A. Koh, Clathrate Hydrates of Natural Gases, CRC, 2008.
[13] U.C. Klomp, V.C. Kruka, R. Reijnhart, WO Patent Application 95/17579, 1995.
[14] U.C. Klomp, V.R. Kruka, R. Reijnhart, A.J. Weisenborn, Method for inhibiting the plugging of conduits by gas hydrates, US Patent 5648575, 1997.
[15] U.C. Klomp, R. Reijnhart, Method for inhibiting the plugging of conduits by gas hydrates, US Patent 5879561, 1999.
[16] U.C. Klomp, Method for inhibiting the plugging of conduits by gas hydrates, US Patent 6152993, 2000.
[17] V. Panchalingam, M.G. Rudel, S.H. Bodnar, Methods for inhibiting hydrate blockage in oil and gas pipelines using amide compounds, US Patent 7381689, 2008.
[18] J.D. York, A. Firoozabadi, Journal of Physical Chemistry B 112 (3) (2008) 845–851.

[19] J.D. York, A. Firoozabadi, Journal of Physical Chemistry B 112 (34) (2008) 10455–10465.
[20] J.D. York, A. Firoozabadi, Energy & Fuels 23 (2009) 2937–2946.
[21] X. Li, L. Negadi, A. Firoozabadi, Energy Fuels 24 (2010) 4937–4943.
[22] M. Sun, Y. Wang, A. Firoozabadi, Energy & Fuels 26 (9) (2012) 5626–5632.
[23] S.Q. Gao, Energy & Fuels 23 (2009) 2118–2121.
[24] H. Moradpour, A. Chapoy, B. Tohidi, Fuel 90 (11) (2011) 3343–3351.
[25] S. Paria, K.C. Khilar, Advances in Colloid and Interface Science 110 (3) (2004) 75–95.
[26] D.M. Nevskaia, A. Guerrero-Ruiz, J. de D. Lopez-Gonzalez, Journal of Colloid and Interface Science 205 (1) (1998) 97–105.
[27] E.D. Sloan, S. Subramanian, P.N. Matthews, J.P. Lederhos, A.A. Khokhar, Industrial & Engineering Chemistry Research 37 (8) (1998) 3124–3132.
[28] J. Emsley, Chemical Society Reviews 9 (1) (1980) 91–124.
[29] P. Somasundaran, S. Krishnakumar, Colloids and Surfaces A: Physicochemical and Engineering Aspects 123 (1997) 491–513.
[30] H.A. Waxman, E.J. Markey, D. DeGette, Chemicals Used in Hydraulic Fracturing, United States House of Representatives, 2011.